HHS Public Access

Author manuscript

Nat Methods. Author manuscript; available in PMC 2016 September 01.

Published in final edited form as:

Nat Methods. 2016 March ; 13(3): 263–268. doi:10.1038/nmeth.3735.

A near-infrared genetically targetable and activatable photosensitizer

Jianjun He[1], **Yi Wang**[2], **Maria A. Missinato**[4], **Ezenwa Onuoha**[4], **Lydia A. Perkins**[2], **Simon C. Watkins**[5], **Claudette M. St. Croix**[5], **Michael Tsang**[4], and **Marcel P. Bruchez**[1,2,3]

[1]Department of Chemistry, Carnegie Mellon University, Pittsburgh, Pennsylvania 15213, USA

[2]Department of Biological Sciences, Carnegie Mellon University, Pittsburgh, Pennsylvania 15213, USA

[3]Molecular Biosensor and Imaging Center, Carnegie Mellon University, Pittsburgh, Pennsylvania 15213, USA

[4]Department of Developmental Biology, University of Pittsburgh School of Medicine, Pittsburgh, Pennsylvania 15213, USA

[5]Center for Biologic Imaging, Department of Cell Biology, University of Pittsburgh; Pittsburgh, Pennsylvania 15213, USA

Abstract

Upon illumination, photosensitizer molecules produce reactive oxygen species (ROS) that can be utilized for functional manipulation of living cells, including protein inactivation, targeted damage introduction, and cellular ablation. Photosensitizers used to date have been either exogenous, resulting in delivery and removal challenges, or genetically encoded proteins that form or bind a native photosensitizing molecule, resulting in a constitutively active photosensitizer inside the cell. By binding a heavy-atom substituted fluorogenic dye with a genetically encoded Fluorogen Activating Protein (FAP), we demonstrate an ‘on-demand’ activated photosensitizer that produces singlet oxygen and fluorescence only when FAP-bound and activated with near infrared light. This Targeted and Activated Photosensitizer (TAPs) approach enables protein inactivation and targeted cell killing in cultured cells and rapid targeted lineage ablation in living larval and adult zebrafish. The near-infrared excitation and emission of this FAP-TAPs photosensitizer module provides a new spectral range for photosensitizer proteins, useful for imaging, manipulation and cellular ablation deep within living organisms.

INTRODUCTION

Light provides precise temporal and spatial control of biological processes, when combined with suitable genetic constructs or chemical reagents[1–3]. Photosensitizer dyes and proteins

Correspondence should be addressed to M.P.B. (bruchez@cmu.edu).

J. H. designed and performed experiments, analyzed data and wrote the paper. Y.W. provided cell culture, performed experiments and wrote the paper. E.O. M.A.M & M. T. developed and provided zebrafish lines, designed and performed experiments and analyzed data. L.A.P. provided reagents. S.C.W and C.M.C performed experiments and analyzed data. M.P.B. designed experiments, analyzed data and wrote the paper.

exploit the absorbed light to create short-lived reactive oxygen species (ROS) that can mediate biological effects precisely and acutely at the target site[4, 5]. Although widely used for many years, traditional photosensitizers such as methylene blue have no selectivity for particular cells or sub-cellular compartments; and the off-target phototoxicity produced during light exposure has constrained the range of applications[6, 7]. Many of these photosensitizers are limited by low photostability, chemical instability, or solubility in biological milieu[8]. Newer photosensitizers with high ROS generating efficiency, good photostability, and near-infrared (NIR) absorption enhanced optical tissue penetration, and allowed real-time fluorescent visualization[9]. More recently, genetically targeted photosensitizers, including FlAsH and ReAsH, KillerRed and MiniSOG[10–13], have been developed to improve targeting and specificity in living cells. These fluorescent photosensitizers display good chromophore-assisted light inactivation (CALI) of directly linked proteins. Genetic fusion allows the photosensitizing protein to produce ROS at the target, selectively inactivating it and allowing study of the resulting changes. These photosensitizer proteins require a very high light dose to reach effective inactivation or cell killing, and the spectral properties of these sensitizers overlap with biological chromophores, resulting in some ROS generation even in the absence of the photosensitizer proteins. For deep tissue applications, and to avoid autofluorescent photosenstization, genetically encoded photosensitizers with far-red/NIR excitation wavelengths (> 620 nm) are required, yet no efficient genetically targeted photosensitizers are presently available in this spectral range.

Photosensitizers that are activated for ROS generation at the target site show improved specificity by minimizing the damage to the surrounding non-targeted tissues, where the photosensitizer remains inactive[14]. Currently, activatable photosensitizers are either responsive to local environmental changes such as pH or hydrophilicity, or contain a quenching group that is cleaved, releasing an active photosensitizer[15–17]. These activation events typically increase the ROS production by 10–50-fold, providing enhanced photosensitizing contrast, but still showing some off-target effects from nonspecifically localized materials. Selectively targeting and significantly activating a photosensitizer at a site of interest remains a significant goal to advance photosensitizer dyes and proteins.

To target and activate a ROS-generating photosensitizer, we exploited a genetically targetable and highly efficient fluorescence-enhancing tag, the fluorogen activating protein (FAP)[18]. FAPs display thousands-fold fluorescence activation, rapid and high-affinity association and high specificity for cognate ligands. Fluorogen-FAP complexes have been adapted to a number of distinct applications with modified dyes, including single molecule imaging[19], physiological pH measurements during receptor endocytosis[20], and protein detection as recombinant affinity probes[21]. In particular, FAP_{dL5**} is a tandem dimer of a double-mutant (E52D, L91S) of the parent L5-MG FAP (reported previously as MBIC5 or dL5**), a 25 kDa binder for malachite green derivatives (MG) with thousands-fold fluorescence activation, low pM dissociation constant, and robust function in various compartments of living cells[18, 22]. We reasoned that the suppression of nonradiative relaxation of the electronic excited state by which the FAP enhances fluorescence in MG fluorogens could be exploited to modify other photochemical properties, in particular intersystem crossing, when combined with chemically tailored fluorogens[23]. We prepared an iodine substituted MG analog with low free fluorescence and ROS generation, that binds to

dL5**, producing a NIR excitable fluorescent complex with high singlet oxygen quantum yield (Figure 1A). This dye -protein complex can be exploited to inactivate fused proteins, to selectively photosensitize cells expressing dL5** at the plasma membrane, cytosol, mitochondrial matrix or nucleus in culture, and to ablate cardiac cells within living larval/adult zebrafish expressing dL5** in the cytoplasm, all with NIR excitation. The free dye shows no photosensitization in cells or zebrafish, indicating that the iodinated MG analog is a potent, NIR excitable, FAP-Targeted and Activated Photosensitizer (TAPs).

RESULTS

MG-2I/dL5** as a singlet oxygen specific photosensitizer

We found that heavy atom substitutions at some sites on the MG chromophore, which are expected to increase intersystem crossing[24, 25], preserved high affinity dL5** binding and desirable optical properties (Supplementary Figure 1). In particular, the di-iodinated MG analog methylium, bis[4-(dimethylamino)phenyl](4 -(3-carboethoxypropyl)-3,5-diiodo-phenyl)-chloride (MG-2I), a derivative of the cell-permeable MG-ester fluorogen, dramatically increased the yield of singlet oxygen when formed as the MG-2I/dL5** complex (FAP-TAPs). The iodination also resulted in a 22nm bathochromic shift of the major absorption band, moving the excitation maximum of the complex into the NIR range (666nm) (Table 1 and Figure 1B). The generation of singlet oxygen was evaluated by bleaching of anthracene-9,10-dipropionic acid (ADPA), a commonly used singlet oxygen scavenger[26], relative to aluminum phthalocyanine tetrasulfonate ($AlPcS_4$) as the standard[27]. The singlet oxygen quantum yield (Φ_Δ) of the FAP-TAPs was determined to be 0.13 (Table 1 and Figure 1C), while the singlet oxygen generation from the MG-ester/dL5** or free TAPs dye were not detectable under the same conditions. We have also compared the ADPA bleaching efficiency using different excitation filters for commonly used fluorescent proteins (Supplementary Figure 2A, 2B), both YFP and RFP excitation show little singlet oxygen production, suggesting the use of these fluorescent proteins is compatible with FAP-TAPs. In deuterated PBS buffer, the bleaching rate of ADPA by FAP-TAPs was significantly enhanced (at 30s, 86% ADPA was bleached by FAP-TAPs in dPBS while only 27% in PBS). Since D_2O is known to increase the lifetime of $^1O_2$ (4μs to 52μs)[28] while exerting little effect on other ROS, the increase in ADPA bleaching seen in deuterated buffer further supports the production of singlet oxygen (Supplementary Figure 3A). Diaminobenzidine (DAB) was successfully photooxidized to produce brown precipitate *in vitro*, potentially useful for Correlative Light and Electron Microscopy (CLEM) (Supplementary Figure 3C). Importantly, neither fluorescence nor singlet oxygen production was detected using free MG-2I dye under normal excitation conditions, even in deuterated PBS, due to the very short excited state lifetime (< 1ps). Comparing ADPA bleaching in deuterated PBS between MG-2I (prolonged exposure) and MG-2I/dL5** complex, binding of the MG-2I results in a >100-fold enhanced Φ_Δ (Supplementary Figure 3B). Coupled with the shift in absorption maximum upon binding, the singlet oxygen generation efficiency for a fixed concentration of dye at the excitation maximum of the complex could be increased up to 450-fold upon binding to the dL5** protein. This ensures that free dye is both non-fluorescent and non-photosensitizing, a critical difference compared to other dye-targeting or photosensitizer-activating approaches. Moreover, with NIR excitation, FAP-TAPs could be used for

simultaneous *in vivo* visualization and ablation with good fluorescence and optical tissue penetration.

FAP-TAPs mediated CALI of the PLC δ1 PH domain

To assess FAP-TAPs utility for targeted protein inactivation, we compared release from the membrane of EGFP-PH-KillerRed and EGFP-PH-dL5** fusion proteins upon suitable illumination in HEK 293 cells[10]. When the pleckstrin homology (PH) domain from PLC δ1 is inactivated by CALI, it translocates from the membrane to the cytoplasm, increasing the cytoplasmic/membrane EGFP signal. As shown in figure 2, after 5min illumination with 560nm (60× objective, 2.03W/cm^2), the cytoplasm-to-membrane signal ratio changed 37% under KillerRed-mediated CALI, similar to previous reports. The fluorescence of KillerRed is significantly bleached (>75%) after 1min illumination. In contrast, FAP-TAPs illumination resulted in a 33% ratio change after 10 s of 640 nm laser illumination (60× objective, 2.07W/cm^2). Further illumination of FAP-TAPs induced no EGFP ratio change but noticeable morphology change and minor photobleaching. The potential collateral damage was also assayed by co-expressing EGFP-PH with PH-KillerRed/PH-dL5**. Although the timescales of illumination were ~30-fold different, both KillerRed and FAP-TAPs induced similar inactivation of EGFP-PH in proportion to the amount of target inactivation, indicating the FAP-TAPs are spatially restricted similarly to KillerRed under CALI conditions. The high efficacy and specificity of FAP-TAPs mediated protein inactivation could facilitate well-controlled, rapid dynamic experiments based on acute protein inactivation, when proximal collateral damage can be properly controlled.

FAP-TAPs mediated cellular photoablation

The light-induced cytotoxicity of FAP-TAPs was evaluated on HEK293 cells expressing a cell-surface anchored FAP (dL5**-TM HEK), where the FAP was anchored in the plasma membrane by a single PGFR-derived transmembrane helix. A mixed population of dL5**-TM expressing and wild-type HEK cells was incubated with 400nM of MG-ester or MG-2I dye for 30 minutes and then illuminated with a continuous laser source (40× objective, 640nm excitation, 0.76W/cm^2) for 1 minute. Only fluorescently labeled TM-dL5** HEK cells that were treated with MG-2I and light were stained dead within 30 minutes using a LIVE/DEAD cell viability kit, while the wild-type HEK cells in the illumination field remained alive and metabolically active (Figure 3A). The labeled cells began to lose cell morphology with swelling and blebbing within a very short period upon illumination (Supplementary Movie 1). MG-ester bound to TM- dL5** HEK cells, MG-2I treated WT HEK cells and non-targeted MG-2I/dL5** complex added to the media showed no apparent cytotoxicity or phototoxicity upon illumination (Figure 3A). These results revealed that close contact of FAP-TAPs on target cells was critical for effective delivery of ROS due to the very short radius of action of singlet oxygen. These results clearly established the dual requirements of targeted FAP expression and activated TAPs recognition in order to achieve efficient photosensitization. Limited self-bleaching (< 30%) was observed during photosensitization (the first minute of continuous illumination) of FAP-TAPs (Supplementary Movie 2), allowing high ROS dose delivery and real time monitoring of site targeting. Under prolonged illumination times, WT HEK cells that are adjacent to FAP-TAPs expressing cells begin to lose viability (Figure 3B). The high photostability of the FAP-TAPs

allows a high degree of tuning in the delivered ROS dose, allowing illumination conditions that selectively kill only expressing cells or prolonged exposures that extends the phototoxicity to nearby, non-targeted cells. dL5** targeted to the cytosol, mitochondria and nuclei of HEK cells successfully induced phototoxicity from the FAP-TAPs (Supplementary Figure 4) at distinct subcellular locations. Use of KillerRed targeted mitochondria has been reported to allow effective cell killing by inducing apoptosis[10, 29]. KillerRed expressed in the mitochondria of HEK cells required 90 minutes of 560nm laser illumination (60× objective, 2.03W/cm^2) to induce 50% effective cell killing, and higher light doses required to achieve 100% killing resulted in significant killing of neighboring non-expressing cells. Using the same laser power, mitochondrially targeted FAP-TAPs illuminated for 90 seconds induced 100% effective cell killing, without damage to neighboring cells (Supplementary Table 1). The light dose required for cellular ablation is at least 60-fold lower than KillerRed. The photostability of the FAP-TAPs, coupled with the ability to induce phototoxic effects regardless of subcellular location distinguishes the performance of this genetically encoded photosensitizer from that of KillerRed and MiniSOG, both of which rapidly photobleach and require expression at specific subcellular locations to exert a potent phototoxic effect[30, 31]. The low light-dose required for FAP-TAPs photoablation, coupled with the efficient optical penetration of NIR light opens new possibilities for ablation in thick, scattering tissues, and across large numbers of animals simultaneously.

Light-dose-dependent cytotoxicity of FAP-TAPs

Using a custom-built light-box emitting at 669nm (24nm FWHM, 0.089W/cm^2 at specimen, Supplementary Figure 5), we quantitatively determined the light-induced cytotoxicity on TM-dL5** HEK cells with various illumination intensities for 15 minutes or with various illumination durations at 0.089W/cm^2 (Figure 3C). WT HEK cells incubated with MG-2I and TM-dL5** HEK cells labeled with MG-ester showed no detectable light-induced cytotoxicity. The LD_{50} of illumination for FAP-TAPs labeled cells was measured to be 50 J/cm^2 in the light box, in agreement with the value obtained by laser illumination (Supplementary Figure 6A) on the microscope. A linear response was observed with changes in illumination duration, while changes in light intensity revealed a more sigmoidal process, suggesting a threshold ROS-generation rate that is tolerated at lower overall light doses. Similar threshold responses to ROS have also been seen in bacteria and mammalian cells, consistent with a cellular buffering system that can mitigate the effects of some excess toxic ROS[32, 33].

In order to specify the ROS generated by FAP-TAPs in cells, we examined the suppression of FAP-TAPs mediated phototoxicity by adding different ROS quenchers to TM-dL5** HEK cells complexed with MG-2I (Supplementary Figure 6B) using the light-box. Sodium azide, a known selective quencher of singlet oxygen, demonstrated a dose-dependent inhibition of the phototoxic response. The phototoxic effect of FAP-TAPs was almost completely suppressed at a sodium azide concentration of 10mM, consistent with other reports of sodium azide-mediated suppression of cytotoxicity[34]. Meanwhile, no significant suppression of phototoxicity was observed when cells were incubated with high concentrations of catalase (a peroxide quencher, 1000U/mL) or superoxide dismutase (SOD, a superoxide quencher, 500U/mL)[35]. Up to 2000U/mL catalase and 1000U/mL SOD were

used under continuous illumination in a confocal microscope (Supplementary Figure 7), resulting in a modest reduction in dead cell staining, but a persistent loss of viability and metabolic activity. Results from these quenching experiments along with the *in vitro* ADPA bleaching assay indicated that singlet oxygen generated from FAP-TAPs was the primary ROS mediating the observed phototoxic responses.

Singlet oxygen is a highly reactive species, and is known to react with nearby organic molecules to produce secondary peroxide species as initial products, which may then propagate to produce other reactive products and lead to cytotoxicity[36]. Hence, different ROS sensors can be used to identify the cascade generation of ROS after photosensitization with FAP-TAPs. Dihydroethidium (DHE), which reacts with superoxide ($O_2^{\cdot -}$) to form a DNA intercalating fluorescent species (2-hydroxyethidium, 490 nm excitation and 567 nm emission), was used to detect ROS species in HEK cells expressing the FAP-TAPs in the nucleus[37]. The ROS-dependent activation of DHE in the nucleus was only observed when MG-2I with FAP and light were present, but not in control cells or FAP-expressing cells labeled and illuminated in the presence of MG-ester dye (Supplementary Figure 8).

FAP-TAPs mediated cardiac ablation in larval zebrafish

*In viv*o cellular ablation has been used to study cell-niche relationships, cellular roles in development and replacement of damaged cells and tissues in regeneration[38]. Zebrafish (*danio rerio*) is a frequently used vertebrate model organism because it is optically transparent, easily genetically manipulated, and shows conserved developmental processes with other vertebrates[39, 40]. Lineage ablation can be accomplished in zebrafish by tissue specific expression of a bacterial nitroreductase (ntr) and subsequent treatment for ~12–24 h with metronidazole, a prodrug that is reduced in ntr^+ cells to a DNA synthesis inhibitor, resulting in cell death[41]. Because of the rapid zebrafish development, 12–24 hours represents a relatively large ablation timeframe, which can limit the temporal resolution of lineage ablation studies. Given the rapid phototoxic response from targeted cells in culture, we sought to test the timescale of cellular ablation in living larval zebrafish. Transgenic zebrafish lines were produced that expressed a cytoplasmic dL5**-mCerulean3 (dL5**-mCer3) tandem protein under control of the heart-specific *myosin light chain 7* (*myl7*, also known as *cmlc2*) promoter, *Tg(myl7: MBIC5-mCer3)*. Expression of dL5**-mCer3 was confirmed by fluorescence imaging of mCer3 and MG-ester/dL5** or MG-2I/dL5**complexes, and was restricted to the beating heart (Supplementary Figure 9A, Supplemental Movie 3). To test the effectiveness of FAP-TAPs, we treated *Tg(myl7: MBIC5-mCer3)*^{pt22} embryos at 48 hour post fertilization (hpf) with 500 nM fluorogen (MG-2I or MG-ester) for 3 hours followed by 12 minutes laser illumination (659nm, 242mW/cm^2). Immediately after illumination, transgenic zebrafish treated with MG-2I showed no sign of heart beat or blood circulation, while MG-ester treated transgenic larvae and wild-type zebrafish treated with MG-2I were normal (Supplementary Movie 4). At 24 hours post illumination (hpi), we found that photo-treated MG-2I/*Tg*^{pt22} larvae exhibited cardiac edema and lower mCer3 fluorescence (Figure 4A). *Tg*^{pt22} larvae treated with MG-2I and light were developmentally delayed relative to control groups, showing smaller eyes and larger yolk at 96hpi (Supplementary Figure 9B). At 96hpi, no $mCer3^+$ cells were detected from photo-treated MG-2I/*Tg*^{pt22} larvae, indicating that acute loss of *myl7* lineage cells was

not renewed later in development. To evaluate ablation, we used deoxynucleotidyl transferase-mediated deoxyuridinetriphosphate nick end-labeling (TUNEL) assay with anti-GFP antibody for mCer3 to quantify dead cells in whole-mount larvae at 24hpi (Supplementary Figure 10A). Reduced mCer3^{+} cells and an increased number of mCer3^{+}/TUNEL^{+} cells were seen in MG-2I/12min larvae, without any increase in mCer3^{-} cell death compared with MG-ester/12min larvae (Supplementary Figure 10B, 10C) We found a significant increase in the fraction of mCer^{+}/TUNEL^{+} cells in MG-2I/12min group compared to MG-ester/12min group (31% vs 4.4%, $p<0.01$)(Supplementary Figure 10D). Shorter illumination time (4min) of MG-2I/*Tg*^{pt22} larvae leads to reduced specific cytotoxicity, confirming the light-dose dependence of the FAP-TAPs function in expressing cells.

We performed cardiac photoablation experiments in adult zebrafish to investigate the effectiveness of the FAP-TAPs in deep tissue, as damaged cardiac muscle can regenerate through proliferation of pre-exsisting cardiomyocytes[42–44]. *Tg(myl7: MBIC5-mCer3)*^{pt23} zebrafish uniformly express mCer3-dL5** in the heart at the adult stage (Supplementary Figure 11A). Zebrafish were retro-orbitally injected with MG-2I or MG-ester and illuminated for a total of 30 minutes using the LED source described earlier (2.5 W/cm^2 illumination from below the fish) (Supplementary Figure 11B). At 3 days post illumination (dpi), hearts, livers and intestine were extracted and cell death was assessed using TUNEL assay. Increased cell death was observed in the hearts of transgenic zebrafish injected with MG-2I, compared to all the control groups, suggesting the efficiency and specificity of the ablation in deep tissue (Figure 4B). In contrast, no difference of apoptotic rate was observed in livers and intestines between all the treatments (Supplementary Figure 11C), demonstrating cardiac restricted injury. To confirm cardiomyocyte ablation, we extracted the hearts at 5 dpi and stained with Acid Fuchsin Orange G (AFOG) staining that labels the intact cardiac muscle (brown). Transgenic hearts injected with MG-2I showed damaged cardiac structure and a reduction of ventricular cardiac muscle as compared to the controls (Figure 4B). Importantly, no structural defects were observed in livers and intestine (Supplementary Figure 11D). At 5 dpi, only illuminated transgenic zebrafish injected with MG-2I had significantly more proliferating cardiomyocytes (Figure 4B), showing that the ablation inflicts sufficient damage to induce a regenerative response.

DISCUSSION

We have demonstrated a two-component targeted and activated photosensitizing approach that enables robust and specific NIR light-mediated protein inactivation and phototoxicity in FAP expressing cells and living transgenic organisms. In contrast to conventional photosensitizers, the TAPs dye (MG-2I) or FAP (dL5**) alone has no photosensitizing effect until they are bound to each other to form the photosensitizer FAP-TAPs. The activation of photosensitization is achieved by ‘on-demand’ addition of fluorogens to the targeted cells instead of the ‘passive’ cleavage of quenching groups by cellular components employed for most other activation mechanisms. This method allows temporally, spatially and subcellularly controlled, target-specific generation of singlet oxygen. The flexible genetic targeting strategy of the FAP along with efficient activation of ROS generation makes FAP-TAPs an immediately useful tool for targeted cellular ablation and subcellular protein

inactivation, which can potentially be multiplexed with other photosensitizers (e.g. KillerRed and MiniSOG). The fact that the same encoded FAP (dL5**) can be used to bind a non-photosensitizing dye (the MG-ester), allows many studies that rely on imaging to be extended to photosensitization only when the researcher adds the TAPs dye. This alternative labeling strategy can facilitate the selection of stable cells and transgenic animals, which are primed for imaging, photoablation or photosensitization studies, depending on the dye and light-dose employed in the study.

Supplementary Material

Refer to Web version on PubMed Central for supplementary material.

Acknowledgments

This work was supported in part with funds from the National Institutes of Health, Technology Centers for Networks and Pathways program U54GM103529, NIH R21ES025606 and NIH R01EB017268. The authors would like to thank Eric Kelley and Christopher J Bakkenist (University of Pittsburgh) for helpful discussion and guidance on establishing ROS species involved in cellular toxicity. We would also like to thank Emily Drill, Callen T Wallace and Mark A Ross for help in larval zebrafish TUNEL imaging.

References

1. Lavis LD, Raines RT. Bright ideas for chemical biology. Acs Chem Biol. 2008; 3:142–155. [PubMed: 18355003]
2. Levskaya A, Weiner OD, Lim WA, Voigt CA. Spatiotemporal control of cell signalling using a light-switchable protein interaction. Nature. 2009; 461:997–1001. [PubMed: 19749742]
3. Lee HM, Larson DR, Lawrence DS. Illuminating the Chemistry of Life: Design, Synthesis, and Applications of “Caged” and Related Photoresponsive Compounds. Acs Chem Biol. 2009; 4:409–427. [PubMed: 19298086]
4. Dolmans DEJGJ, Fukumura D, Jain RK. Photodynamic therapy for cancer. Nat Rev Cancer. 2003; 3:380–387. [PubMed: 12724736]
5. Jacobson K, Rajfur Z, Vitriol E, Hahn K. Chromophore-assisted laser inactivation in cell biology. Trends Cell Biol. 2008; 18:443–450. [PubMed: 18706812]
6. Allison RR, et al. Photosensitizers in clinical PDT. Photodiagn Photodyn. 2004; 1:27–42.
7. Castano AP, Demidova TN, Hamblin MR. Mechanisms in photodynamic therapy: part one-photosensitizers, photochemistry and cellular localization. Photodiagn Photodyn. 2004; 1:279–293.
8. Rosenthal I. Phthalocyanines as Photodynamic Sensitizers. Photochem Photobiol. 1991; 53:859–&. [PubMed: 1886943]
9. Josefsen LB, Boyle RW. Photodynamic therapy: novel third-generation photosensitizers one step closer? Br J Pharmacol. 2008; 154:1–3. [PubMed: 18362894]
10. Bulina ME, et al. A genetically encoded photosensitizer. Nat Biotechnol. 2006; 24:95–99. [PubMed: 16369538]
11. Shu XK, et al. A Genetically Encoded Tag for Correlated Light and Electron Microscopy of Intact Cells, Tissues, and Organisms. Plos Biol. 2011; 9
12. Westberg M, Holmegaard L, Pimenta FM, Etzerodt M, Ogilby PR. Rational design of an efficient, genetically encodable, protein-encased singlet oxygen photosensitizer. J Am Chem Soc. 2015; 137:1632–1642. [PubMed: 25575190]
13. Tour O, Meijer RM, Zacharias DA, Adams SR, Tsien RY. Genetically targeted chromophore-assisted light inactivation. Nat Biotechnol. 2003; 21:1505–1508. [PubMed: 14625562]
14. Lovell JF, Liu TWB, Chen J, Zheng G. Activatable Photosensitizers for Imaging and Therapy. Chem Rev. 2010; 110:2839–2857. [PubMed: 20104890]

15. McDonnell SO, et al. Supramolecular photonic therapeutic agents. J Am Chem Soc. 2005; 127:16360–16361. [PubMed: 16305199]
16. Zheng G, et al. Photodynamic molecular beacon as an activatable photosensitizer based on protease-controlled singlet oxygen quenching and activation. Proc Natl Acad Sci U S A. 2007; 104:8989–8994. [PubMed: 17502620]
17. Tian JW, et al. Cell-Specific and pH-Activatable Rubyrin-Loaded Nanoparticles for Highly Selective Near-Infrared Photodynamic Therapy against Cancer. J Am Chem Soc. 2013; 135:18850–18858. [PubMed: 24294991]
18. Szent-Gyorgyi C, et al. Fluorogen-activating single-chain antibodies for imaging cell surface proteins (vol 26, pg 235, 2008). Nat Biotechnol. 2008; 26:470–470.
19. Saurabh S, et al. Multiplexed Modular Genetic Targeting of Quantum Dots. Acs Nano. 2014; 8:11138–11146. [PubMed: 25380615]
20. Grover A, et al. Genetically Encoded pH Sensor for Tracking Surface Proteins through Endocytosis. Angew Chem Int Edit. 2012; 51:4838–4842.
21. Saunders MJ, Block E, Sorkin A, Waggoner AS, Bruchez MP. A Bifunctional Converter: Fluorescein Quenching scFv/Fluorogen Activating Protein for Photostability and Improved Signal to Noise in Fluorescence Experiments. Bioconjugate Chem. 2014; 25:1556–1564.
22. Szent-Gyorgyi C, et al. Malachite Green Mediates Homodimerization of Antibody V-L Domains to Form a Fluorescent Ternary Complex with Singular Symmetric Interfaces. J Mol Biol. 2013; 425:4595–4613. [PubMed: 23978698]
23. Koziar JC, Cowan DO. Photo-Chemical Reactions .15. Photo-Chemical Heavy-Atom Effects. Accounts Chem Res. 1978; 11:334–341.
24. Gandin E, Lion Y, Vandevorst A. Quantum Yield of Singlet Oxygen Production by Xanthene Derivatives. Photochem Photobiol. 1983; 37:271–278.
25. Yogo T, Urano Y, Ishitsuka Y, Maniwa F, Nagano T. Highly efficient and photostable photosensitizer based on BODIPY chromophore. J Am Chem Soc. 2005; 127:12162–12163. [PubMed: 16131160]
26. Lindig BA, Rodgers MAJ, Schaap AP. Determination of the Lifetime of Singlet Oxygen in D_2O Using 9,10-Anthracenedipropionic Acid, a Water-Soluble Probe. J Am Chem Soc. 1980; 102:5590–5593.
27. Davila J, Harriman A. Photosensitized Oxidation of Biomaterials and Related Model Compounds. Photochem Photobiol. 1989; 50:29–35. [PubMed: 2762381]
28. Ogilby PR. Singlet oxygen: there is indeed something new under the sun. Chem Soc Rev. 2010; 39:3181–3209. [PubMed: 20571680]
29. Shibuya T, Tsujimoto Y. Deleterious effects of mitochondrial ROS generated by KillerRed photodynamic action in human cell lines and C. elegans. J Photoch Photobio B. 2012; 117:1–12.
30. Qi YCB, Garren EJ, Shu XK, Tsien RY, Jin YS. Photo-inducible cell ablation in Caenorhabditis elegans using the genetically encoded singlet oxygen generating protein miniSOG. Proc Natl Acad Sci U S A. 2012; 109:7499–7504. [PubMed: 22532663]
31. Williams DC, et al. Rapid and Permanent Neuronal Inactivation In Vivo via Subcellular Generation of Reactive Oxygen with the Use of KillerRed. Cell Rep. 2013; 5:553–563. [PubMed: 24209746]
32. Patterson MS, Wilson BC, Graff R. Invivo Tests of the Concept of Photodynamic Threshold Dose in Normal Rat-Liver Photosensitized by Aluminum Chlorosulfonated Phthalocyanine. Photochem Photobiol. 1990; 51:343–349. [PubMed: 2356229]
33. Schafer M, et al. Systematic study of parameters influencing the action of Rose Bengal with visible light on bacterial cells: Comparison between the biological effect and singlet-oxygen production. Photochem Photobiol. 2000; 71:514–523. [PubMed: 10818781]
34. Kuimova MK, Yahioglu G, Ogilby PR. Singlet Oxygen in a Cell: Spatially Dependent Lifetimes and Quenching Rate Constants. J Am Chem Soc. 2009; 131:332–340. [PubMed: 19128181]
35. Tilly JL, Tilly KI. Inhibitors of Oxidative Stress Mimic the Ability of Follicle-Stimulating-Hormone to Suppress Apoptosis in Cultured Rat Ovarian Follicles. Endocrinology. 1995; 136:242–252. [PubMed: 7828537]
36. Simon HU, Haj-Yehia A, Levi-Schaffer F. Role of reactive oxygen species (ROS) in apoptosis induction. Apoptosis. 2000; 5:415–418. [PubMed: 11256882]

37. Zhao HT, et al. Superoxide reacts with hydroethidine but forms a fluorescent product that is distinctly different from ethidium: Potential implications in intracellular fluorescence detection of superoxide. Free Radical Bio Med. 2003; 34:1359–1368. [PubMed: 12757846]

38. Fuchs Y, Steller H. Programmed Cell Death in Animal Development and Disease (vol 147, pg 742, 2011). Cell. 2011; 147:1640–1640.

39. Dodd A, Curtis PM, Williams LC, Love DA. Zebrafish: bridging the gap between development and disease. Hum Mol Genet. 2000; 9:2443–2449. [PubMed: 11005800]

40. Lieschke GJ, Currie PD. Animal models of human disease: zebrafish swim into view. Nat Rev Genet. 2007; 8:353–367. [PubMed: 17440532]

41. Curado S, Stainier DY, Anderson RM. Nitroreductase-mediated cell/tissue ablation in zebrafish: a spatially and temporally controlled ablation method with applications in developmental and regeneration studies. Nat Protoc. 2008; 3:948–954. [PubMed: 18536643]

42. Poss KD, Wilson LG, Keating MT. Heart regeneration in zebrafish. Science. 2002; 298:2188–2190. [PubMed: 12481136]

43. Kikuchi K, et al. Primary contribution to zebrafish heart regeneration by gata4(+) cardiomyocytes. Nature. 2010; 464:601–U162. [PubMed: 20336144]

44. Jopling C, et al. Zebrafish heart regeneration occurs by cardiomyocyte dedifferentiation and proliferation. Nature. 2010; 464:606–U168. [PubMed: 20336145]

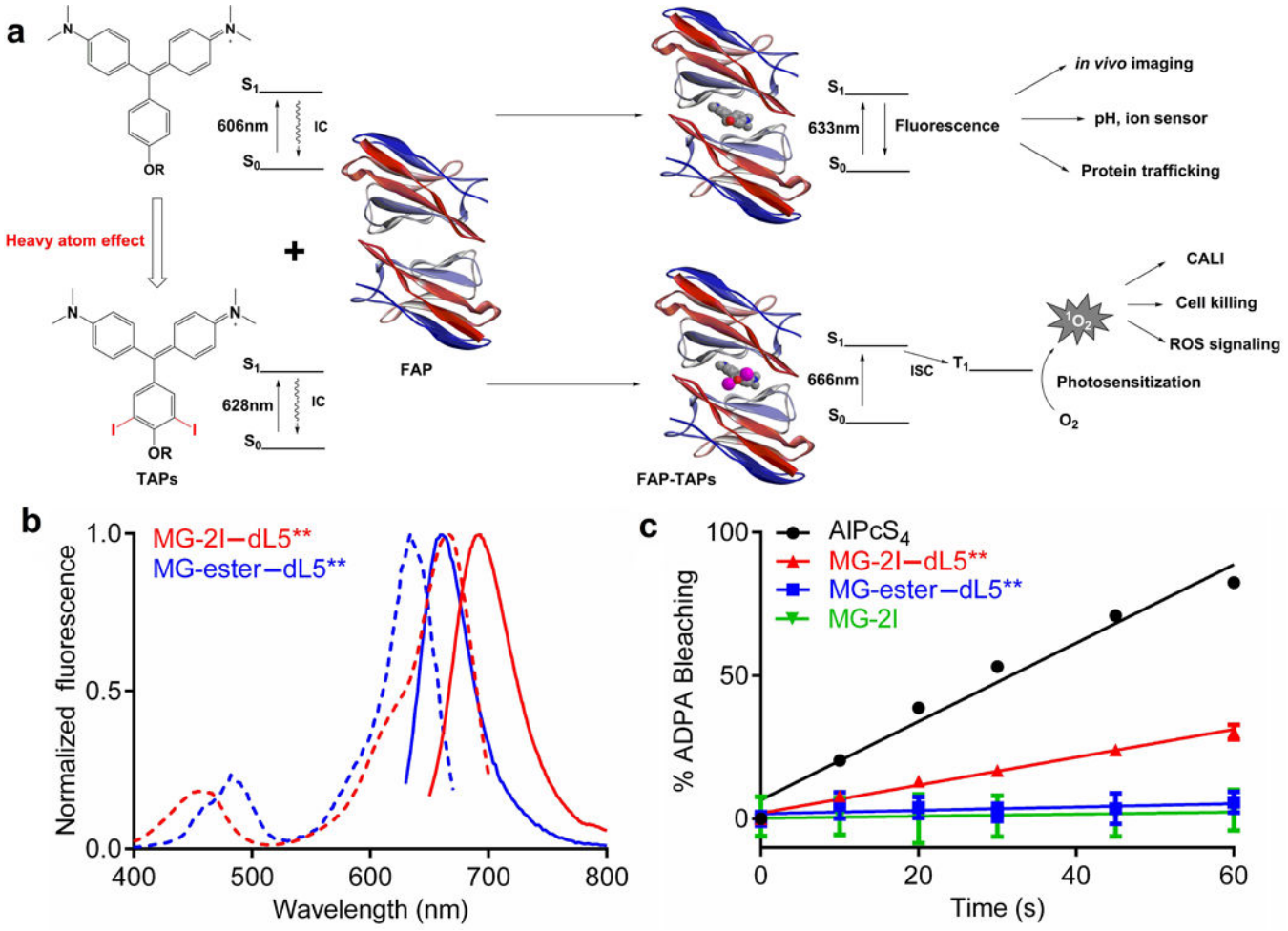

Figure 1.

Characterization of ROS generation by FAP-TAPs. (**a**) Illustration of the ROS generating mechanism of FAP-TAPs. IC: internal conversion by molecule's free rotation, ISC: intersystem crossing; (**b**) Normalized excitation (dotted lines) and emission (solid lines) spectra of MG-ester and MG-2I binding to dL5**, where 500 nM fluorogen was complexed with 3 μM dL5** and the fluorescence intensity was individually normalized to the peak maxima; (**c**) Measurement of $^1O_2$ generation by MG-2I–dL5** by ADPA, where bleaching of ADPA fluorescence was monitored at 374/402 nm as a function of 669 nm exposure time. $AlPcS_4$ was used as standard for the $^1O_2$ generation (Φ_Δ= 0.34). Optically matched solutions of MG-2I–dL5** and $AlPcS_4$ at 669 nm were used. (n = 4, mean and S.E.M. plotted)

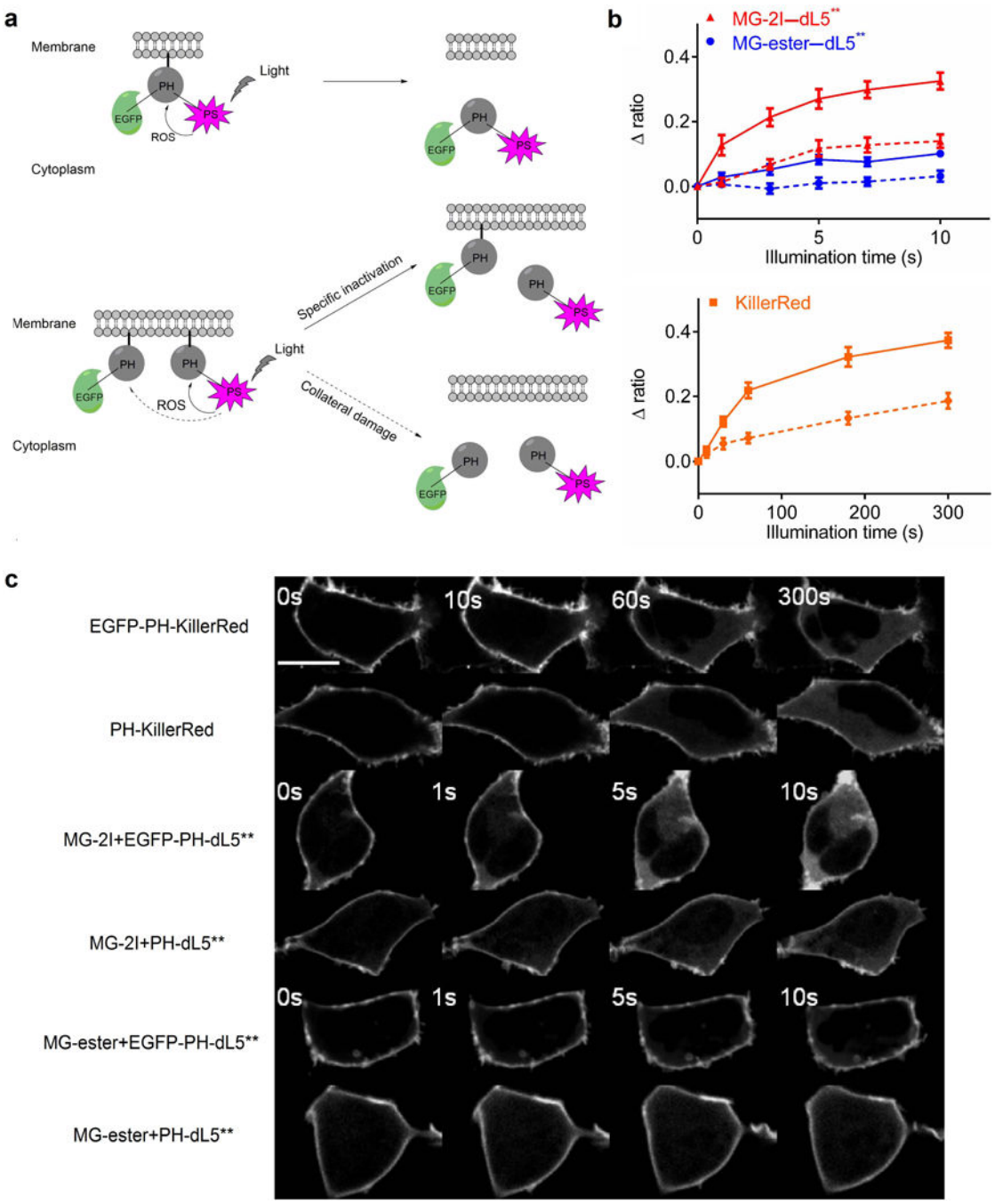

Figure 2.

FAP-TAPs mediated light-induced protein inactivation of the PLC δ1 PH domain. (**a**) Schematic outline of the experimental design. Top: EGFP-PH-KillerRed or EGFP-PH-dL5** triple fusion protein was constructed to evaluate the effectiveness of specific protein inactivation from KillerRed and FAP-TAPs. Bottom: EGFP-PH was co-expressed with PH-KillerRed or PH-dL5** to estimate the collateral damage from KillerRed and FAP-TAPs; (**b**) EGFP cytoplasm to membrane ratio change upon illumination of MG-2I with EGFP-PH-dL5**, MG-ester with EGFP-PH-dL5** and EGFP-PH-KillerRed (Solid lines). Dashed

lines are corresponding collateral damage from co-expressed proteins; (n = 8, mean and S.E.M. plotted) (**c**) Representative EGFP fluorescent signal change from each condition, with imaging at fixed intervals. Scale bar = 5 μm and applied to all images. Illumination condition: KillerRed: 560 nm laser, 60× objective, 2.03 W cm^{-2}; MG-ester–dL5** and MG-2I–dL5**: 640 nm laser, 60× objective, 2.07 W cm^{-2}.

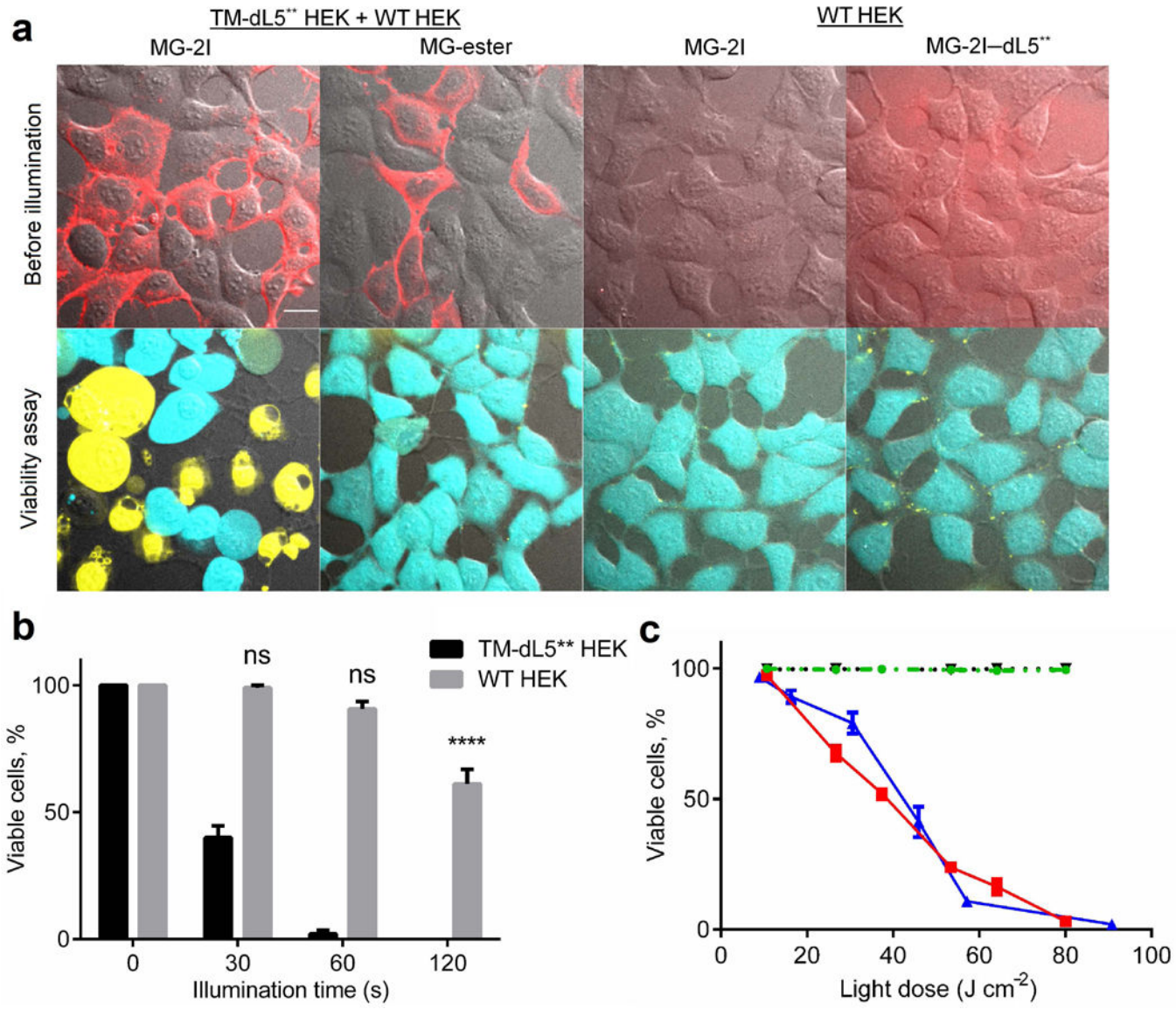

Figure 3.

Phototoxicity of FAP-TAPs on HEK cells expressing surface targeted FAP. Cells were labeled with 400 nM of the indicated dye 30 min prior to illumination, without removal of the unbound dye. (**a**) Photo-induced cell death required both the binding of MG-2I to dL5** and the cellular targeting of the complex. Top panel: images taken before laser illumination, merge of c640 (red) and DIC; bottom panel: Live/Dead cell viability assay 30 min after illumination, merge of c488 (live cells in cyan), c560 (dead cells in yellow) and DIC. Scale bar = 10 μm and applied to all images; (**b**) Collateral damage to WT HEK cells caused by TAPs targeted to TM-dL5** HEK cells. A mixture of TM-dL5** and WT HEK cells were subjected to 0 s, 30 s, 60 s and 120 s illumination (640 nm, 40× objective, 0.76 W cm^{-2}), the viability of TM-dL5** and WT HEK cells were plotted above (n = 8, One-way ANOVA, Tukey post hoc tests were performed with multiple comparisons, mean and S.E.M. plotted); (**c**) Light dose dependent cytotoxicity is seen on TM-dL5** cells labeled with MG-2I under

variable light intensity (blue) or variable illumination duration (red). In contrast, no phototoxic effect is seen for MG-ester with TM-dL5** HEK cells (dotted black) or MG-2I with WT HEK cells (dashed green). Cells were illuminated using a LED light box. Cells were stained with propidium iodide (dead) and Hoechst (total) and over 300 cells were counted for each data point (n = 4, mean and S.E.M. plotted).

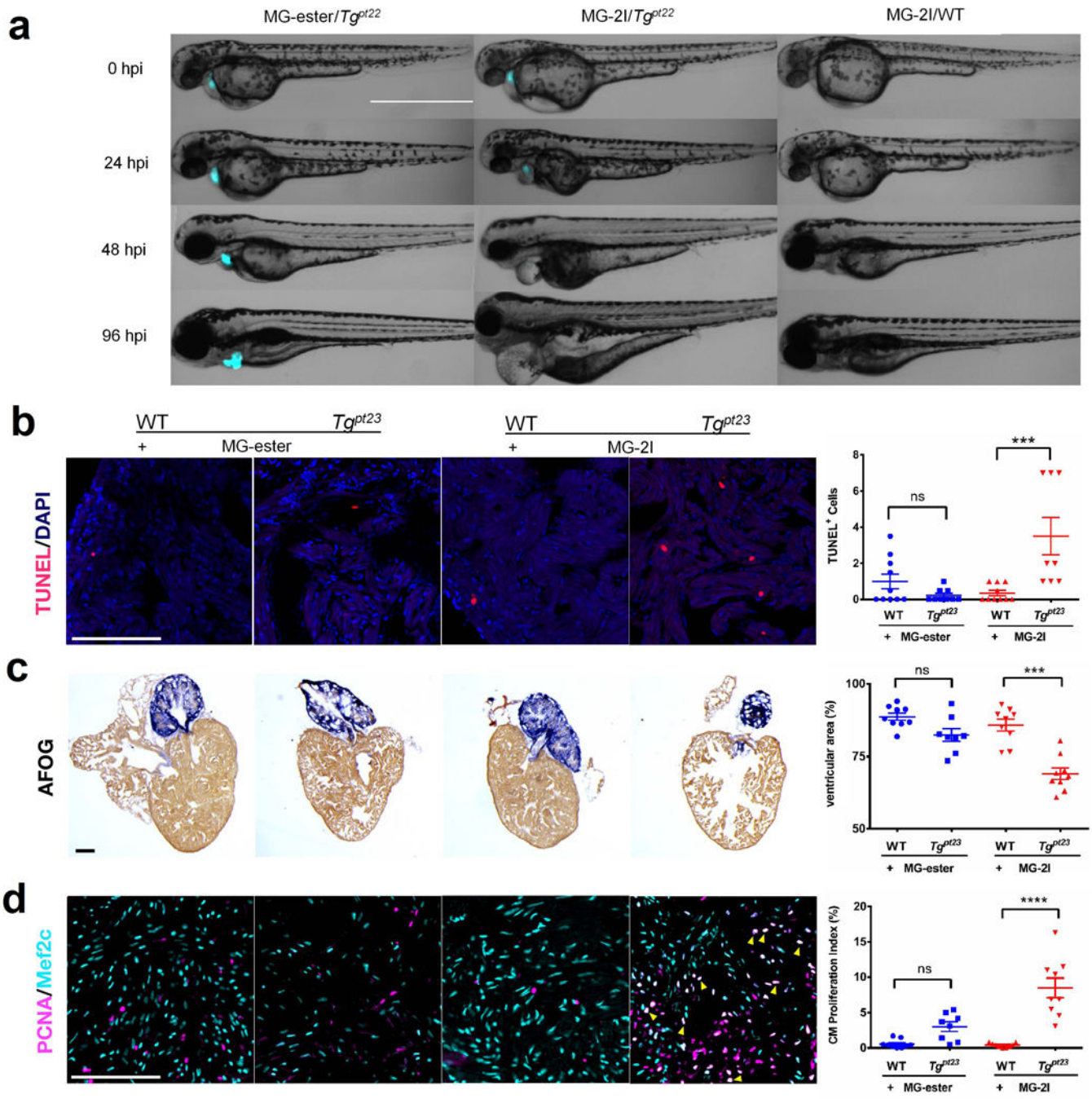

Figure 4.

FAP-TAPs induced photo-ablation of cardiac function. (a) Phenotype development from 0 hpi to 96 hpi of larval zebrafish (Merge of DIC and mCer3 fluorescence (cyan), n = 20 for each group): MG-ester/*Tg*^{pt22}, MG-2I/*Tg*^{pt22} and MG-2I/WT. In MG-2I/*Tg*^{pt22} group, the larvae developed a range of visible defects: large cardiac edema, small eyes, and collapsed, nonfunctional heart chambers. In both control groups, development proceeded normally. Scale Bar = 1000 μm and applied to all images; (b) FAP-TAPs photo-induced cardiac damage in adult zebrafish. Hearts were extracted at 3 dpi and TUNEL was performed to

assess cell death; (c) Acid Fuchsin Orange G (AFOG) staining of hearts at 5 dpi showing the damaged cardiac structure in transgenic fish injected with MG-2I; (d) Mef2c (cardiomyocyte) and PCNA (proliferation) staining at 5 dpi shows enhanced cardiomyocyte proliferation (yellow arrow) in transgenic fish injected with MG-2I. Scale bar = 100 μm and applied to all images, n = 9 for all groups, One-way ANOVA, Tukey post hoc tests were performed with multiple comparisons of mean for each group. *P*-values were considered significant when < 0.05, shown as mean ± S.E.M.

Table 1

Summary of spectral, FAP binding and ROS generating properties between MG-ester and MG-2I complexed with dL5**, KillerRed is listed as a comparison.

Complex	λ_{Abs} [a] (nm)	λ_{ex} (nm)	λ_{em} (nm)	K_d (pM)	ε_{max} [b] (10^4 $M^{-1}cm^{-1}$)	Φ_F	Φ_Δ	DAB photoconversion
MG-ester–dL5**	606	633	668	7	10.3(9.18)	0.12	<0.005	−
MG-2I–dL5**	628	666	693	122	10.1(9.02)	0.037	0.13	+++
KillerRed	585	585	610	NA	4.5	0.25	0	−

[a] Values are respective absorption maximum of fluorogen only;

[b] The values in parentheses are for the unbound fluorogen at its respective maximum.